Nuclear Factor I-C Is Essential for Odontogenic Cell Proliferation and Odontoblast Differentiation during Tooth Root Development*

Dong-Seol Lee[‡]**, Jong-Tae Park**[‡]**, Hyun-Man Kim**[‡]**, Jea Seung Ko**[‡]**, Ho-Hyun Son**[§]**, Richard M. Gronostajski**[¶]**, Moon-Il Cho**[∥]**, Pill-Hoon Choung**[**‡‡]**, and Joo-Cheol Park**[‡1]

From the [‡]Department of Oral Histology-Developmental Biology, Dental Research Institute, [§]Conservative Dentistry, [**]Oral & Maxillofacial Surgery, and [‡‡]Tooth Bioengineering National Research Lab, School of Dentistry, Seoul National University, Seoul 110-749, Korea and the [¶]Department of Biochemistry and the Program in Neuroscience, School of Medicine and Biomedical Science, and the [∥]Department of Oral Biology, School of Dental Medicine, State University of New York at Buffalo, Buffalo, New York 14214-3092

Our previous studies have demonstrated that nuclear factor I-C (NFI-C) null mice developed short molar roots that contain aberrant odontoblasts and abnormal dentin formation. Based on these findings, we performed studies to elucidate the function of NFI-C in odontoblasts. Initial studies demonstrated that aberrant odontoblasts become dissociated and trapped in an osteodentin-like mineralized tissue. Abnormal odontoblasts exhibit strong bone sialoprotein expression but a decreased level of dentin sialophosphoprotein expression when compared with wild type odontoblasts. Loss of *Nfic* results in an increase in p-Smad2/3 expression in aberrant odontoblasts and pulp cells in the subodontoblastic layer *in vivo* and primary pulp cells from *Nfic*-deficient mice *in vitro*. Cell proliferation analysis of both cervical loop and ectomesenchymal cells of the *Nfic*-deficient mice revealed significantly decreased proliferative activity compared with wild type mice. In addition, *Nfic*-deficient primary pulp cells showed increased expression of p21 and p16 but decreased expression of cyclin D1 and cyclin B1, strongly suggesting cell growth arrest caused by a lack of *Nfic* activity. Analysis of the pulp and abnormal dentin in *Nfic*-deficient mice revealed an increase in apoptotic activity. Further, *Nfic*-deficient primary pulp cells exhibited an increase in caspase-8 and -3 activation, whereas the cleaved form of Bid was hardly detected. These results indicate that the loss of *Nfic* leads to the suppression of odontogenic cell proliferation and differentiation and induces apoptosis of aberrant odontoblasts during root formation, thereby contributing to the formation of short roots.

Tooth development is a complex and well coordinated developmental process that is achieved through a series of reciprocal interactions between dental epithelium and neural crest-derived ectomesenchyme (EM).[2] The dental epithelium gives rise to the outer and inner enamel epithelium from which ameloblasts differentiate, whereas EM cells differentiate into odontoblasts. The critical roles of several transcription factors and growth factors in crown formation have been well documented (1, 2). After completion of crown formation, the inner and outer enamel epithelial cells proliferate and form Hertwig's epithelial root sheath that plays a key role in root formation. It is believed, based on information derived from crown development, that Hertwig's epithelial root sheath induces the differentiation of EM cells from the radicular pulp area into odontoblasts that are responsible for root dentin formation. However, the molecular mechanisms responsible for root development are not well understood (3–5).

The nuclear factor I (NFI) family of transcription/replication factors was first discovered as a family of proteins required for the replication of adenovirus DNA *in vitro* (6). The NFI gene family encodes site-specific transcription factors essential for the development of a number of organ systems (7). There are four NFI gene family members in vertebrates (*Nfia*, *Nfib*, *Nfic*, and *Nfix*) and a single NFI gene in *Drosophila melanogaster* and *Caenorhabditis elegans* (*Nfi-1*) (7, 8). The consequences of individual gene disruptions in mice of each of the four *Nfi* genes have been reported. *Nfia*-deficient mice exhibit defects in brain development (9), whereas *Nfib*-deficient mice show defects in lung maturation and brain development (10, 11). *Nfix*-deficient mice reveal defects in brain and skeleton development (12). Interestingly, *Nfic*-deficient mice demonstrate normal molar crown formation but aberrant odontoblast differentiation during root formation as well as short root formation and severe incisor defects (13). However, the exact roles of NFI-C in root formation remain unknown.

Transforming growth factor (TGF)-β, a prominent member of the TGF-β superfamily of ligands including TGF-βs,

[1] To whom correspondence should be addressed: School of Dentistry, Seoul National University, 28, Yeonkun-Dong, Chongro-Ku, Seoul, 110-749, Korea. Tel.: 82-2-740-8668; Fax: 82-2-763-3613; E-mail: jcapark@snu.ac.kr.

[2] The abbreviations used are: EM, ectomesenchyme; NFI-C, nuclear factor I-C; TGF, transforming growth factor; TGFβ-RI, transforming growth factor β receptor I; BSP, bone sialoprotein; DSP, dentin sialoprotein; DSPP, dentin sialophosphoprotein; RNAi, RNA interference; PBS, phosphate-buffered saline; P*n*, postnatal day *n*; BrdU, 5'-bromo-2'-deoxyuridine; TUNEL, terminal deoxynucleotidyltransferase-mediated dUTP nick end labeling; RT, reverse transcription; MTT, 3-(4,5-dimethylthiazol-2-yl)-2,5-diphenyltetrazolium bromide, a tetrazole; FGF, fibroblast growth factor; IAP, inhibitor of apoptosis.

activins, and bone morphogenetic proteins, regulates a broad spectrum of biological responses in a variety of cell types (14, 15). The exposure of cells to TGF-β1 can trigger a variety of cellular responses including cell growth arrest, differentiation, and apoptosis (16, 17). Upon binding of TGF-β1 to the TGF-β receptor II, the TGF-β receptor I (TGFβ-RI) is recruited and phosphorylated. The activated TGFβ-RI then phosphorylates Smad2 and Smad3 and forms a complex with a common partner, Smad4, which translocates into the nucleus to act as a transcriptional regulator (18). During mouse tooth development, TGF-β1 has been implicated as a key mediator in odontoblast differentiation and dentin mineralization (19). Interestingly, conditional overexpression of TGF-β1 in mouse odontoblasts under the control of the dentin sialophosphoprotein (DSPP) promoter revealed the same phenotypic changes as seen in *Nfic*-deficient mice. These include the presence of aberrant odontoblasts and their entrapment in abnormal dentin (20). Further, treatment with TGF-β1 of immortalized preodontoblastic MDPC-23 cells derived from a mouse molar dental papilla (21, 22) induced the expression of Smad2, Smad3, Smad4, and apoptosis (23).

In the present study, we sought to determine whether odontoblasts change phenotypically into osteoblasts in *Nfic*-deficient mice. Further, we investigated whether disruption of the *Nfic* gene causes cell growth arrest and apoptosis of odontoblasts. Finally, we determined the molecular mechanism for cell growth arrest of odontogenic cells and apoptosis in *Nfic*-deficient odontoblasts.

EXPERIMENTAL PROCEDURES

Antibodies—Antisera against NFI-C, DSP, and BSP (24) were produced by immunization of rabbit with the synthetic peptides NH$_2$-RPTRPLQTVPLWD-COOH (amino acid residues 427~439 of NFI-C), NH$_2$-GNKSIITKESGKLSGS-COOH (amino acid residues 372~387 of DSP), and NH$_2$-RRIKAED-SEENGVFKYR-COOH (amino acid residues 24~40 of BSP). Mouse monoclonal anti-cyclin D1 (antibody 2926) and rabbit polyclonal anti-p16 (antibody 4824) were purchased from Cell Signaling Technology. All other antibodies, against TGFβ-RI (sc-398), p-Smad2/3 (sc-11769), p21 (sc-6246), cyclin B1 (sc-752), caspase-8 (sc-7890), caspase-3 (sc-7148), Bid (sc-11423), and cIAP1/2 (sc-12410) were purchased from Santa Cruz Biotechnology.

Plasmid Constructs—RNAi NFIC plasmid (pLKO.1-NFIC small hairpin RNA) and control plasmid (pLKO.1) were purchased from Open Biosystems. pCH-NFIC expression plasmid was provided by Dr. R. M. Gronostajski (State University of New York at Buffalo, Buffalo, NY). Full-length Samd2 and Smad3 expression plasmid and a BSP promoter (pGL3LUC-2478~+60) plasmid were kind gifts from Dr. H.-M. Ryoo (Department of Cell and Developmental Biology, School of Dentistry and Dental Research Institute, Seoul National University, Seoul, Korea). The DSPP promoter (pGL3LUC-791~+54) plasmid was a kind gift from Dr. W.-X. He (Department of Operative Dentistry, Qin Du Stomatological, Xian, China).

Tissue Preparation and Immunohistochemistry—Tissue preparation and immunohistochemistry were performed as described previously (25). Briefly, the mice were cardiac-perfused with 4% paraformaldehyde-phosphate-buffered saline (PBS), their heads were removed, and then they were decalcified in a 10% EDTA (pH 7.4) solution at 4 °C and processed for embedding in paraffin. The deparaffinized sections were immersed in 0.6% H$_2$O$_2$/methanol for 20 min to quench the endogenous peroxidase activity. They were then preincubated with 1% bovine serum albumin in PBS for 30 min and incubated overnight at 4 °C with rabbit polyclonal DSP, BSP (1:100), or p-Smad2/3 (1:200; Santa Cruz Biotechnology) antibodies. Sections were incubated for 1 h at room temperature with the secondary antibody and reacted with avidin-biotin-peroxidase complex (Vector Laboratories) in PBS for 30 min. After color development with 0.05% 3,3'-diaminobenzidine tetrahydrochloride (Vector Laboratories), the sections were counterstained with hematoxylin.

Primary Pulp Cell Culture—The mandibles were removed from 17-day-old (P17) wild type and *Nfic*-deficient mice, and primary cell culture was conducted as described before (26). Briefly, after the incisors were dissected out, they were cracked longitudinally using a 27-gauge needle on a 1-ml syringe. The pulp tissues were removed gently with forceps, cut into several pieces, and placed on 60-mm culture dishes (Nunc). The explants were weighed down with a sterile cover glass and cultured in Dulbecco's modified Eagle's medium (Invitrogen) supplemented with 100 IU/ml penicillin, 100 IU/ml streptomycin (Invitrogen), and 10% fetal bovine serum (Invitrogen). The cells were cultured at 37 °C in a humidified atmosphere containing 5% CO$_2$, and cells at passage 2 were used in the experiments.

BrdUrd Staining for Cell Proliferation—Proliferating cells were detected immunohistochemically after intraperitoneal injection of BrdUrd (50 mg/kg of body weight; Sigma-Aldrich). The mice were sacrificed at 4 h after BrdUrd injection, and their heads were removed and processed for embedding in paraffin as described above. BrdUrd-labeled cells in 5-μm-thick sections were then identified using a BrdUrd staining kit (Zymed Laboratory) according to the manufacturer's instructions and counterstained with hematoxylin. The labeling indices for BrdUrd-immunopositive cervical loop and EM cells were obtained.

TUNEL POD Staining—Apoptotic cells were detected in paraffin sections using a terminal deoxynucleotidyl transferase-mediated dUTP nick end labeling (TUNEL) kit (In Situ Cell Death Detection Kit, POD) according to the manufacturer's instructions (Roche Applied Science). The endogenous peroxidase within the tissue sections was inactivated by incubation for 10 min in 3% H$_2$O$_2$ before enzymatic labeling. TUNEL POD staining was achieved by incubation with 3,3'-diaminobenzidine tetrahydrochloride after enzymatic labeling, and sections were counter-stained with methyl green.

Reverse Transcription (RT)-PCR and Real Time PCR Analysis—Total RNA was extracted from the primary pulp cells with TRIzol® reagent according to the manufacturer's instructions (Invitrogen). Total RNA (2 μg) was subjected to reverse transcription with 0.5 μg of oligo(dT) and 1 μl (50 IU) of Superscript III enzyme (Invitrogen) in a 20-μl reaction mixture at 50 °C for 1 h. The resulting mixture was amplified by PCR. One microliter of the reverse transcription product was subjected to

TABLE 1
Nucleotide sequences of real time PCR primer pairs

Gene	Primer (5′ → 3′)
NFIC	
Forward	GACCTGTACCTGGCCTACTTTG
Reverse	CACACCTGACGTGACAAAGCTC
DSPP	
Forward	ATTCCGGTTCCCCAGTTAGTA
Reverse	CTGTTGCTAGTGGTGCTGTT
BSP	
Forward	CAGGGAGGCAGTGACTCTTC
Reverse	AGTGTGGAAAGTGTGGCGTT
DMP1	
Forward	CATTCTCCTTGTGTTCCTTTGGG
Reverse	TGTGGTCACTATTTGCCTGTG
Nestin	
Forward	CCCTGAAGTCGAGGAGCTG
Reverse	CTGCTGCACCTCTAAGCGA
OC	
Forward	CTGACAAAGCCTTCATGTCCAA
Reverse	GCGCCGGAGTCTGTTCACTA
Collagen type I	
Forward	GCTCCTCTTAGGGGCCACT
Reverse	CCACGTCTCACCATTGGGG
TGF-β1	
Forward	CTCCCGTGGCTTCTAGTGC
Reverse	GCCTTAGTTTGGACAGGATCTG
TGF-β3	
Forward	CCTGGCCCTGCTGAACTTG
Reverse	TTGATGTGGCCGAAGTCCAAC
HPRT	
Forward	CCTAAGATGAGCGCAAGTTGAA
Reverse	CCACAGGGACTAGAACACCTGCTA

PCR using the following cycling conditions: 94 °C for 0.5 min; 55 °C for 0.5 min; and 72 °C for 1 min for 32 cycles. The forward and reverse primers were as follows: 5′-GAC CTG TAC CTG GCC TAC TTT G-3′ and 5′-TTT CCA CCA AAA ATG CAG GCT GG-3′ for *NFI-C* and 5′-ATG TGG AAA TGG ATA CTG AC-3′ and 5′-CTA TGT TTG GAT CGT CAT GG-3′ for *Fgf10*. As the quantitative control, glyceraldehyde-3-phosphate dehydrogenase PCR (forward 5′-ACC ACA GTC CAT GCC ATC AC-3′ and reverse 5′-TCC ACC ACC CTG TTG CTG T-3′) was also performed for 20 or 25 cycles using the same cycle profile as used for *NFI-C*. The PCR products were electrophoresed on a 1.2% agarose gel, stained with ethidium bromide, and visualized under UV light.

For real time PCR, specific primers for NFIC, DSPP, BSP, DMP1, nestin, osteocalcin, collagen type I, TGF-β1, TGF-β3, and HPRT were synthesized as listed in Table 1. Real time PCR was performed on an ABI PRISM 7500 sequence detection system with SYBR GREEN PCR Master Mix (Applied Biosystems) according to the manufacturer's instructions. The PCR conditions were 94 °C for 1 min followed by 95 °C for 15 s and 62 °C for 34 s for 40 cycles. All of the reactions were run in triplicate and were normalized to the housekeeping gene HPRT. The evaluation of relative difference of PCR results was calculated by using the comparative cycle threshold (C_T) method.

MTT Assay for Cell Proliferation—The proliferation of primary pulp cells was evaluated using the MTT assay. Primary pulp cells were seeded on 48-well plates at a density of 5×10^3 cells/well and cultured. After washing with PBS, 50 μl of MTT (5 mg/ml) was added to each well and incubated for 4 h at 37 °C. After removing the MTT solution, the converted dye was dis-

solved in Me_2SO and measured by reading the absorbance at a wavelength of 540 nm with a microplate reader (Multiskan EX; Thermo Electron corporation). Triplicate samples were analyzed from three independent experiments.

MDPC-23 Cell Culture—MDPC-23 cells (a generous gift from Drs. C. T. Hanks and J. E. Nör, School of Dental Medicine, University of Michigan, MI) were grown and maintained in Dulbecco's modified Eagle's medium (Invitrogen) supplemented with 10% fetal bovine serum (Invitrogen) and antibiotics (penicillin G, 100 units/ml; streptomycin, 100 μg/ml; and fungizone, 2.5 μg/ml; Invitrogen) at 5% CO_2 in a 37 °C incubator.

Luciferase Assay—MDPC-23 cells were seeded in a 24-well plate at a density of 1×10^5 cells/well. After 24 h, the cells were transfected with the Lipofectamine Plus™ reagent (Invitrogen) according to the manufacturer's instructions. For each transfection, 0.4 μg of the luciferase reporter plasmid, and where indicated, 0.4 μg of the expression vector were used. The vectors were pGL3basic, pLKO.1 (control), RNAi NFIC (si NFIC), pCH-NFI-C (NFIC-over), Smad2, and Smad3 expression plasmid. The cells were also incubated for 48 h with 10 ng/ml of TGF-β1 (R & D Systems). After 48 h of transfection, the cells were lysed for luciferase activity assessment using the luciferase reporter gene assay system (Roche Applied Science) according to the manufacturer's instructions. The measurements were performed with a luminometer (FLUOStar OPTIMA; BMC Laboratory).

Flow Cytometric Analysis for DNA Content—MDPC-23 cells were transiently transfected with the Lipofectamine Plus™ reagent in Opti-MEM (Invitrogen) containing 2 μg of the control vector (pLKO.1 control) or RNAi NFIC plasmid (pLKO.1-NFIC small hairpin RNA). Transfections were performed according to the manufacturer's instructions. The cell cycle was analyzed by flow cytometric quantification of the DNA contents after propidium iodide staining. After 72 h, the cells were trypsinized, washed in PBS, and fixed in 70% ethanol. For cell cycle analysis, the cells were suspended in PBS containing propidium iodide (10 μg/ml) and RNase A (2 μg /ml) for 30 min at room temperature and analyzed by FACScalibur flow cytometry (BD Bioscience, San Jose, CA).

Western Blot Analysis—To prepare whole cell extracts, the cells were washed three times with PBS, scraped into 1.5-ml tubes, and pelleted by centrifugation at 1,000 × *g* for 5 min at 4 °C. After removal of the supernatant, the pellet was resuspended in lysis buffer (100 mM Tris, pH 7.4, 350 mM NaCl, 10% glycerol, 1% Nonidet P-40, 1 mM EDTA, 1 mM dithiothreitol, 10 μg/ml aprotinin, 10 μg/ml leupeptin, and 10 μg/ml pepstatin) and incubated for 15 min on ice. Cell debris was removed by centrifugation at 16,000 × *g* for 15 min at 4 °C. The proteins (30 μg) were separated by 10% SDS-PAGE and transferred onto a nitrocellulose membrane (Schleicher & Schuell). The membranes were blocked for 1 h with 5% nonfat dry milk in PBS containing 0.1% Tween 20 (PBS-T), washed with the PBS-T, and incubated overnight with primary antibody diluted in PBS-T buffer (1:1000) at 4 °C. After washing, the membranes were then incubated with anti-mouse, -rabbit, or -goat IgG-conjugated horseradish peroxidase (Santa Cruz Biotechnology) for 1 h. Labeled protein bands were detected using an enhanced
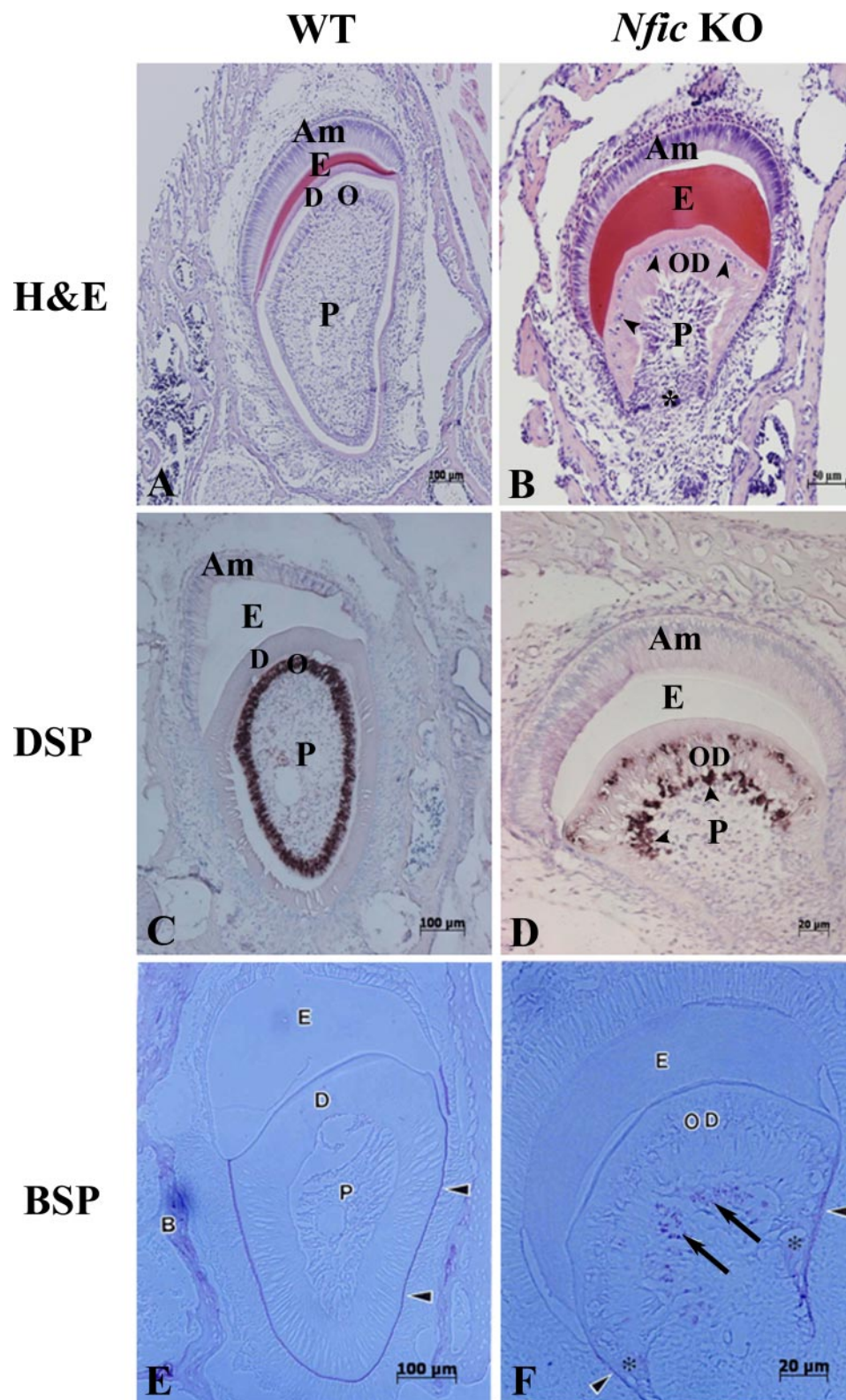
FIGURE 1. **Light micrographs showing cross-sections of P10 incisors from wild type (*WT*) and *Nfic*-deficient (*Nfic KO*) mice.** *A*, a wild type incisor showing a circular ring of dentin and odontoblasts that line the inner surface of dentin. *B*, an *Nfic*-deficient incisor showing an open area (*) caused by the lack of dentin formation caused by abnormal odontoblasts. Note thick osteodentin-like mineralized tissue that contains numerous trapped cells (*arrowheads*) (hematoxylin and eosin-stained, *A* and *B*). Immunohistochemical localization of DSP (*C* and *D*) and BSP (*E* and *F*) in wild type and *Nfic*-deficient incisors is shown. *C*, DSP is strongly expressed in wild type odontoblasts. *D*, DSP is weakly detected in abnormal odontoblasts that are trapped in osteodentin-like mineralized tissue as well as those lining the inner osteodentin-like mineralized tissue (*arrowheads*). *E*, BSP is localized primarily in the cementum (*arrowheads*) along the dentin surface and alveolar bone in wild type incisors. *F*, BSP is observed in cementum (*arrowheads*) along the dentin surface, newly formed osteodentin-like mineralized tissue (*), and areas occupied by abnormal odontoblasts (*arrows*) in *Nfic*-deficient incisors. *Am*, ameloblasts; *E*, enamel; *D*, dentin; *O*, odontoblasts; *OD*, osteodentin-like mineralized tissue; *P*, pulp; *B*, bone. *Scale bars*, *A*, *C*, and *E*, 100 μm; *B*, 50 μm; *D* and *F*, 20 μm.
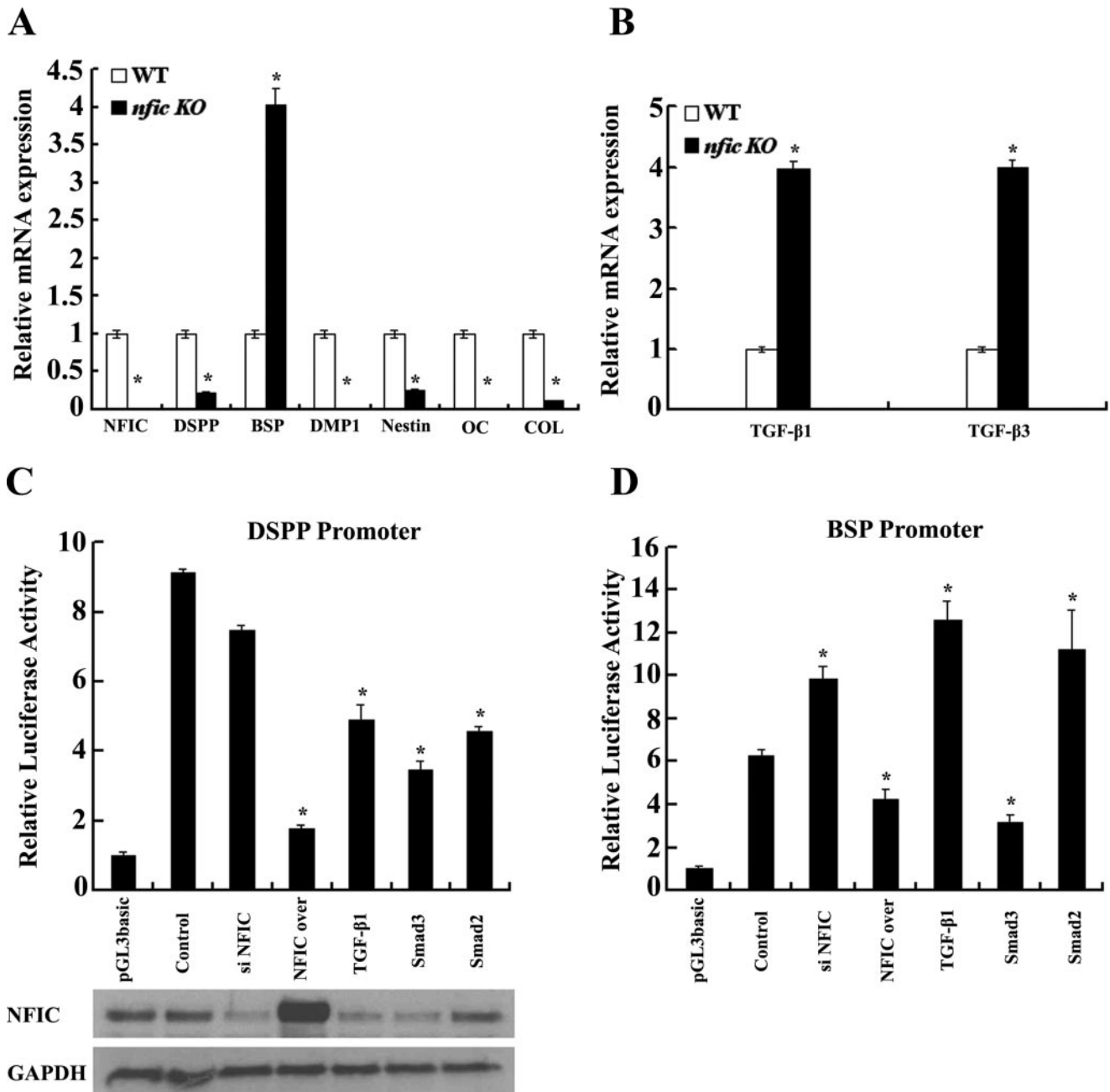
FIGURE 2. **Real time PCR and promoter activity analysis.** Expression of dentin and bone matrix genes (*A*), *TGF-β1*, and *TGF-β3* (*B*) was analyzed by real time PCR in primary pulp cells. DSPP (*C*) and BSP (*D*) promoter activity measured in MDPC-23 cells. The cells were co-transfected with 0.4 μg of pGL3LUC-791$\sim$+54 (DSPP promoter) or pGL3LUC-2744$\sim$+60 (BSP promoter) and pGL3basic, RNAi NFIC (*si NFIC*), pCH-NFIC (*NFIC over*), Smad 2, Smad 3 expression vector, or empty expression vector (pLKO.1, control). The cells were also incubated for 48 with 10 ng/ml of TGF-β1. After 48 of the transfection, promoter activity determined as luciferase light units/protein as expressed as fold activation compared with control activity (co-transfection of empty expression vector) means ± S.D. of three separated experiments. NFIC protein level (*lower panel*) was detected by Western blot 72 h post-transfection as in the *upper panel*. An *asterisk* denotes values significantly different from control by a nonparametric Mann-Whitney test ($p < 0.01$). *COL*, collagen type I. *WT*, wild type.

chemiluminescence system (Amersham Biosciences), and the bands were measured by densitometric analysis of autoradiograph films.

Statistical Analysis—The data were analyzed for statistical significance using a nonparametric Mann-Whitney test.

RESULTS

Histological Analysis of Teeth from Nfic-deficient Mice—To determine whether disruption of the *Nfic* gene causes the phenotypic change of odontoblasts into osteoblasts, we performed light microscopic analysis of morphological changes during EM cell differentiation into odontoblast in wild type and *Nfic*-deficient mice incisors. A cross-section of an incisor from wild type mice showed the presence of circular dentin and odontoblasts that form a layer lining the periphery of the pulp (Fig. 1*A*). However, an incisor from *Nfic*-deficient mice revealed an open area of the dentin caused by the lack of dentin formation. EM cells of *Nfic*-deficient mice incisors failed to differentiate into normal odontoblasts. These abnormal odontoblasts were round in shape, and many of the cells were trapped in osteoden-
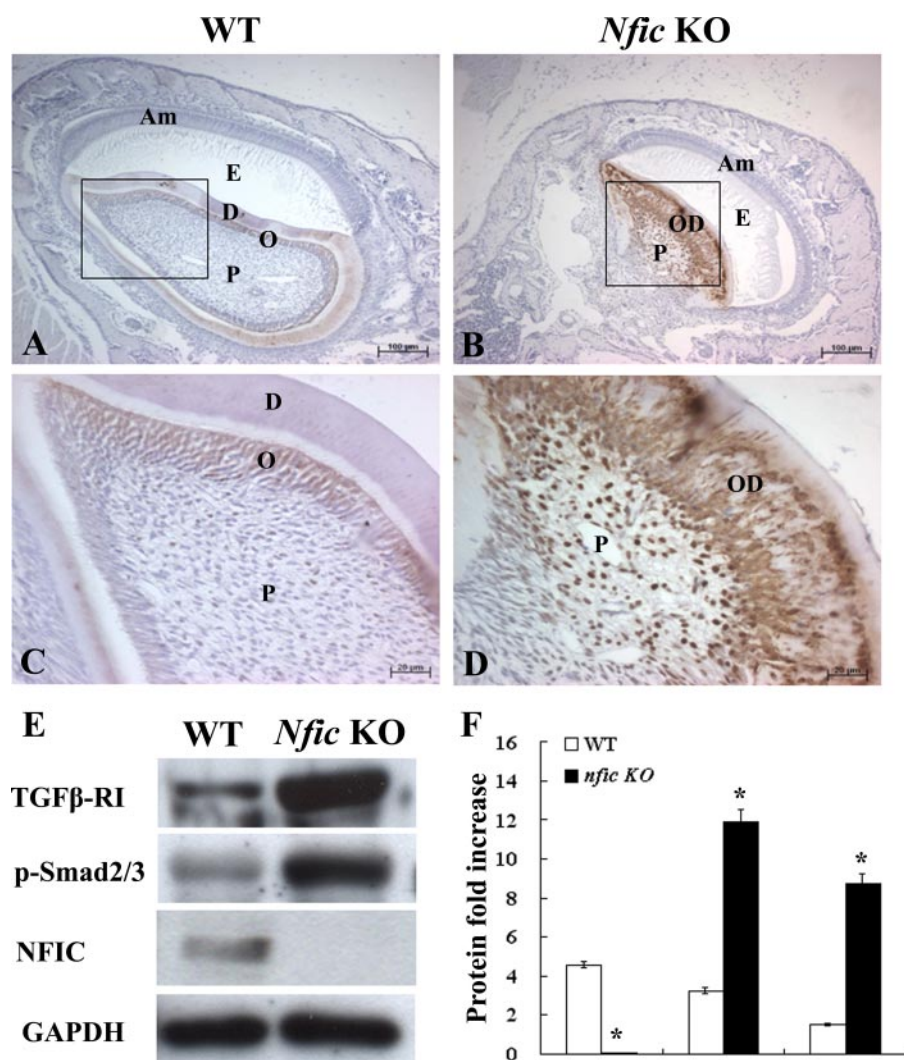
WT   **Nfic KO**

FIGURE 3. **Expression of p-Smad2/3 and TGFβ-RI.** Expression of p-Smad2/3 in P17 incisors from the wild type and *Nfic*-deficient mice was analyzed by immunohistochemistry. p-Smad2/3 was expressed strongly in the incisors of *Nfic*-deficient mice (*B* and *D*) compared with wild type mice (*A* and *C*). *E*, evaluation of TGFβ-RI, p-Smad2/3, and *Nfic* protein expression. Whole cell lysates were purified from primary pulp cells and separated by SDS-PAGE. Western blot analysis was carried out using anti-NFI-C, anti-TGFβ-RI, and anti-p-Smad2/3 antibodies and normalized to glyceraldehyde-3-phosphate dehydrogenase as an internal control. *F*, bands were measured by densitometric analysis of autoradiograph films. An *asterisk* denotes values significantly different between two groups (*p* < 0.05). *C* and *D* are higher magnifications of *A* and *B*, respectively. A sagittal section is shown. *Am*, ameloblasts; *E*, enamel; *D*, dentin; *O*, odontoblasts; *OD*, osteodentin-like mineralized tissue; *P*, pulp. *Scale bars*, *A* and *B*, 50 μm; *C* and *D*, 20 μm.

sion (Fig. 1*D*). This loss of the odontoblast-specific DSP protein suggests an aberrant differentiation state of the embedded cell.

If the aberrant embedded cells resemble osteoblasts, they would be expected to express the osteoblast-specific gene BSP (29). To determine whether the mineralized tissue formed by abnormal odontoblasts in *Nfic*-deficient mice contains BSP, cross-sections of the incisors from wild type and *Nfic*-deficient mice were prepared to compare the immunohistochemical localization of BSP. In wild type incisors, BSP expression was restricted to a thin layer of cementum that covers the dentin but is absent within the dentin (Fig. 1*E*), which is in agreement with a recent finding that cementoblasts in the normal developing roots express BSP mRNA, whereas odontoblasts do not (25). In contrast, strong BSP expression was observed not only in the newly formed mineralized tissue formed by aberrant odontoblasts within *Nfic*-deficient mice incisors but also in the areas where abnormal odontoblasts were located (Fig. 1*F*).

Effect of Loss of Nfic on Dentin and Bone Matrix Gene Expression in Vitro—Dentin and bone matrix gene expression was analyzed by real time PCR in primary pulp cells from wild type and *Nfic*-deficient incisors. DSPP, DMP1, nestin, osteocalcin, and collagen type I expression was decreased in the *Nfic*-deficient primary pulp cells compared with wild type cells (Fig. 2*A*). However, BSP expression was increased in *Nfic*-deficient primary pulp cells (Fig. 2*A*). Additionally, TGF-β1 and TGF-β3 were also up-regulated in the *Nfic*-deficient primary pulp cells (Fig. 2*B*). A previous study has demonstrated that TGF-β1 down-regulates DMP-1 and DSPP genes in odontoblasts (30). Interestingly, a Runx2 transgenic mice study has demonstrated that Runx2 inhibits the terminal differentiation of odontoblasts and that Runx2 induces transdifferentiation of odontoblasts into osteoblasts forming a bone-like structure (31). Collagen type I and DSPP expression was down-regulated, and nestin and osteocalcin expression was severely decreased in the odontoblasts of Runx2 transgenic mice as seen in *Nfic*-deficient mice. These findings suggest that odontoblasts in Runx2 transgenic and *Nfic*-deficient mice lost the phenotype of odontoblasts and acquired those of osteoblasts.
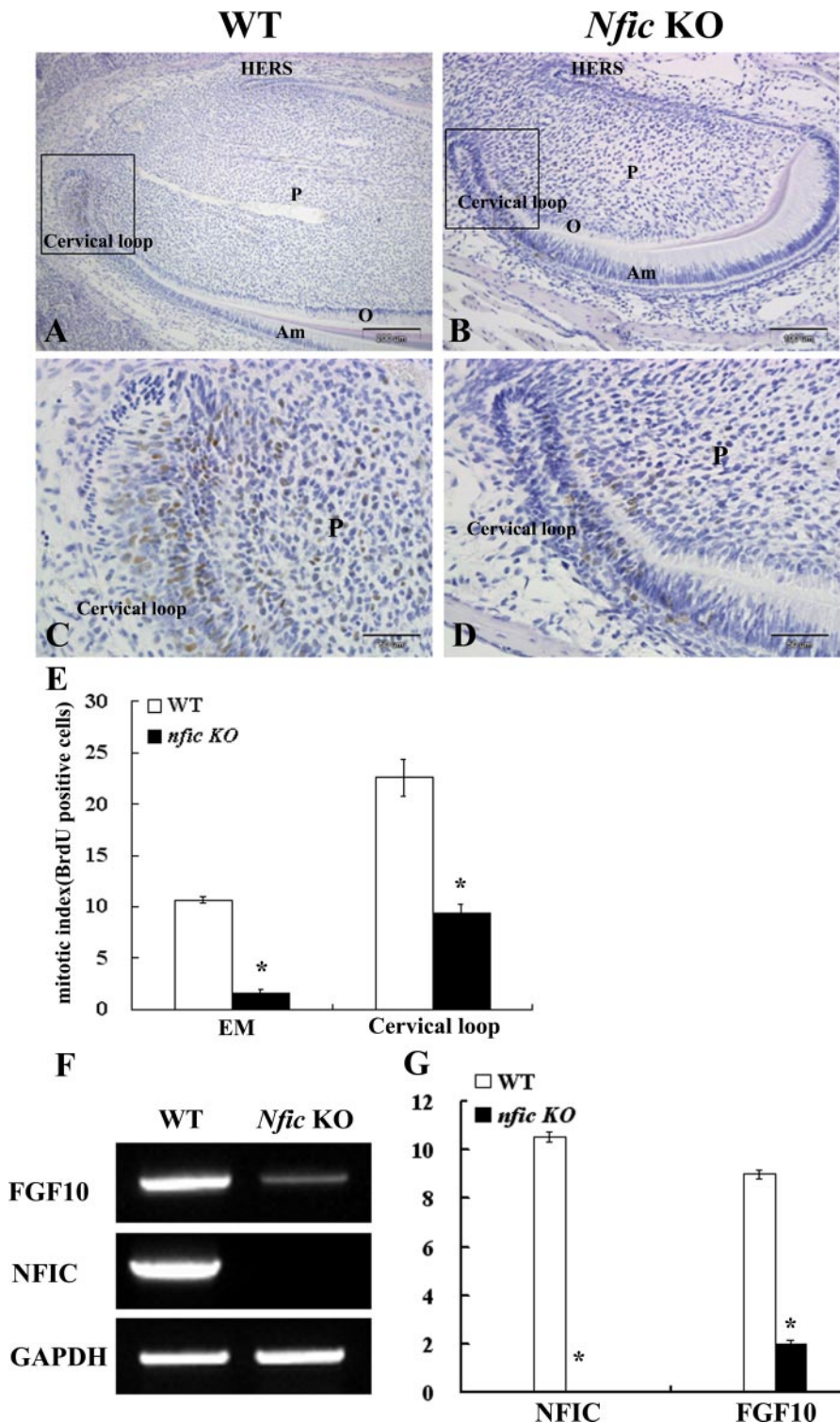
tin-like mineralized tissue and therefore resembled osteocytes (Fig. 1*B*). Osteodentin contains abnormal odontoblasts with a round shape, no odontoblastic processes, and no polarity. With continuous deposition of matrix, they become trapped and form atubular abnormal dentin because it resembles bone in overall morphology (27).

If a phenotypic change from odontoblasts into osteoblasts occurs as a result of the loss of *Nfic*, the abnormal odontoblast-like cells are expected to be looser or have a decreased ability to express the odontoblast-specific gene, DSPP. To test this hypothesis, we performed immunohistochemical analysis of DSP expression in *Nfic*-deficient mice incisors. DSP is a product of DSPP gene (28). Wild type odontoblasts demonstrate strong DSP protein expression (Fig. 1*C*), whereas abnormal odontoblasts exhibited a decreased level of DSP protein expres-

FIGURE 4. Proliferation activity was lower in *Nfic*-deficient mice. Proliferation activity was analyzed by measuring BrdUrd incorporation in the P10 incisors of wild type (*A* and *C*) and *Nfic*-deficient mice (*B* and *D*). *E*, quantification of BrdUrd-labeled cells in the cervical loop and EM cells in the incisors of wild type and *Nfic*-deficient mice. The total number of BrdUrd-positive cells was lower in the cervical loop and EM cells of *Nfic*-deficient mice. *F*, *Fgf10* mRNA expression in primary pulp cells was analyzed by RT-PCR. *G*, bands were measured by densitometric analysis. The data are presented as the means ± S.D. *, $p < 0.05$. *C* and *D* are higher magnifications of boxed *A* and *B*, respectively. A sagittal section is shown. *Am*, ameloblasts; *O*, odontoblasts; *P*, pulp; *EM*, ectomesenchyme. *Scale bars*, *A* and *B*, 50 μm; *C* and *D*, 20 μm.

DSPP and BSP Promoter Activity—TGF-β1 is known to down-regulate DSPP expression (32), whereas it up-regulates BSP expression (33). Therefore, to determine whether disrup-

tion of *Nfic* gene down-regulates DSPP and up-regulates BSP expression because of the up-regulation of TGF-β1, we measured DSPP and BSP promoter activity in MDPC-23 cells. As expected, DSPP promoter activity decreased upon TGF-β1 treatment, as well as when Smad2 and Smad3 were overexpressed compared with untreated cells. Overexpression of *Nfic* also led to a decrease in DSPP promoter activity (Fig. 2*C*). Furthermore, BSP promoter activity increased following small interfering RNA inactivation of *Nfic*, TGF-β1 treatment, or overexpression of Smad2 compared with untreated cells, whereas overexpression of *Nfic* and Smad3 led to a decrease in BSP promoter activity (Fig. 2*D*).

Expression of TGFβ-RI and p-Smad2/3—To understand the mechanism by which the loss of *Nfic* causes short root formation, the expression of p-Smad2/3 was investigated using immunohistochemistry. Although p-Smad2/3 was barely detected in cells extracted from the incisors of wild type mice (Fig. 3, *A* and *C*), it was strongly detected in incisors from *Nfic*-deficient mice (Fig. 3, *B* and *D*). Similar results were also found in the molars from wild type and *Nfic*-deficient mice (data not shown).

To confirm these findings, the expression of the TGFβ-RI and p-Smad2/3 was examined in primary pulp cell cultures from wild type as well as *Nfic*-deficient mice. Western blot analysis revealed a dramatic increase in the expression of TGFβ-RI and p-Smad2/3 in the *Nfic*-deficient primary pulp cells compared with that of wild type (Fig. 3, *E* and *F*).

Cell Proliferation Activity—To determine whether the formation of short roots in *Nfic*-deficient mice is the result of decreased cell proliferation of cervical loop and EM cells, cell proliferation was assessed and compared between wild type and

Nfic-deficient mice using BrdUrd labeling. The number of BrdUrd-labeled cervical loop and EM cells in the incisors of wild type mice (Fig. 4, *A* and *C*) was much higher than that in
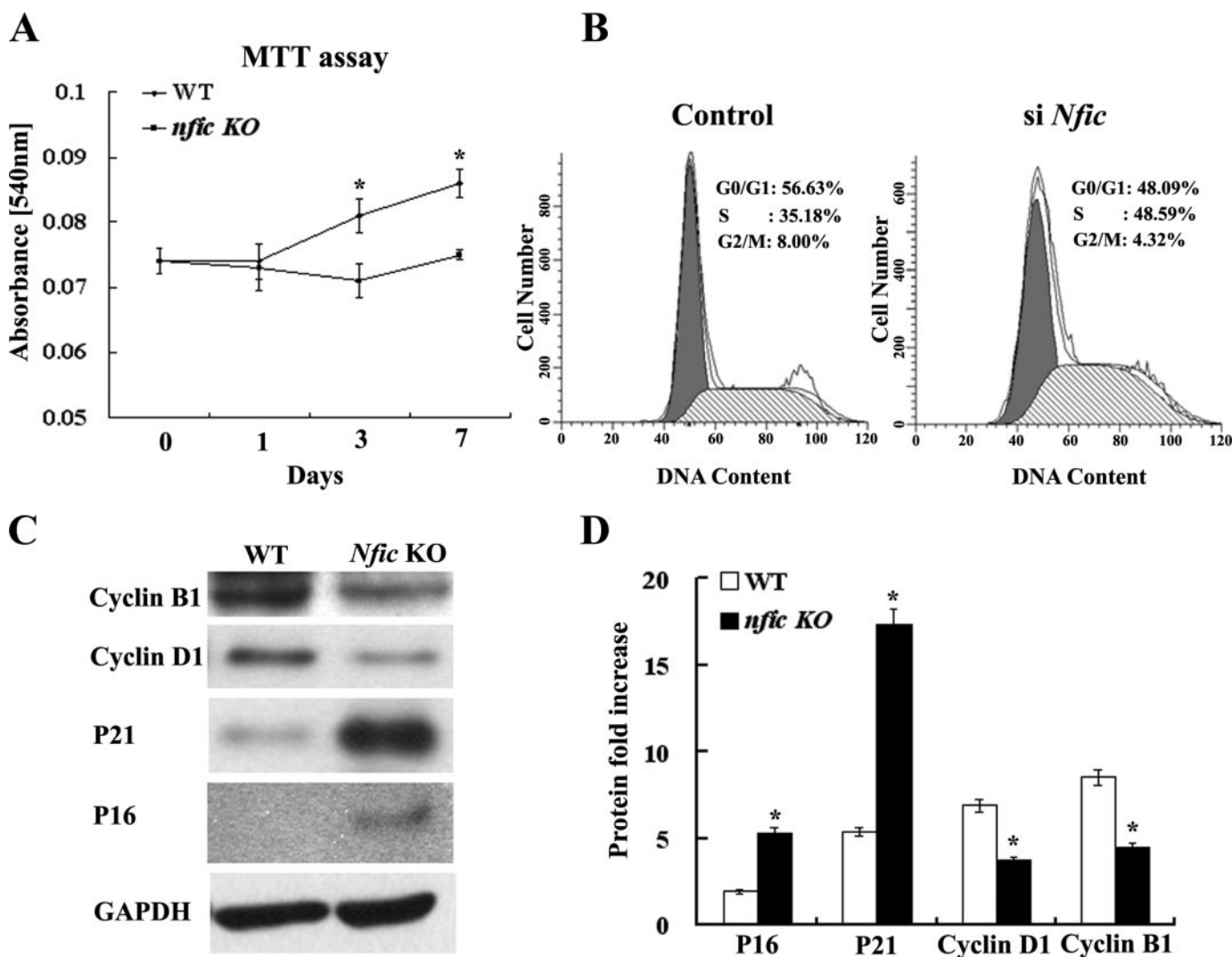
FIGURE 5. **Loss of *Nfic* prevented cell cycle progression caused by p21 overexpression in primary pulp cells.** *A*, cell proliferation assay. Primary pulp cells were seeded on 48-well plates at a density of 5×10^3 cells/well and cultured. Cell proliferation was evaluated by the MTT assay at 1, 3, 5, and 7 days. The data were presented as the means ± S.D. of three independent experiments (*, $p < 0.05$). *B*, flow cytometric analysis of cell growth arrest in MDPC-23 cells. MDPC-23 cells were transiently transfected with 2 μg of the control vector (pLKO.1 control) and RNAi NFIC plasmid (pLKO.1-NFIC small hairpin RNA) as described under "Experimental Procedures." After 72 h, the cells were harvested, fixed with 70% ethanol, and stained with propidium iodide. DNA content was determined by flow cytometry. *C*, evaluation of p21, p16, cyclin D1, and cyclin B1 protein expression. Whole cell lysates were obtained from primary pulp cells and separated by SDS-PAGE. Western blot analysis was carried out using anti-p21, anti-p16, anti-cyclin D1, and anti-cyclin B1 antibodies and normalized to glyceraldehyde-3-phosphate dehydrogenase as an internal control. *D*, bands were measured by densitometric analysis of autoradiograph films (*, $p < 0.05$). *WT*, wild type.

Nfic-deficient mice (Fig. 4, *B* and *D*) and was reduced by 2.5–5-fold in the *Nfic*-deficient mice (Fig. 4*E*).

Previously, it was reported that mouse incisor mesenchymal cells express fibroblast growth factor 10 (FGF10). FGF10 is important for the maintenance of the stem cell niche of the dental epithelium and for the continuous growth of the mouse incisor (34). We therefore examined expression of *Fgf10* by RT-PCR in primary pulp cells. Our data show that *Fgf10* was significantly decreased in *Nfic*-deficient primary pulp cells compared with wild type (Fig. 4, *F* and *G*).

The influence of *Nfic* on cell proliferation was further investigated *in vitro* using the MTT assay. The proliferation rates of *Nfic*-deficient primary pulp cells were found to be decreased by 13% compared with their wild type counterparts when cells were cultured for up to 7 days (Fig. 5*A*).

The influence of *Nfic* on cell cycle control was analyzed by examining the cellular DNA content using a flow cytometer

following propidium iodide staining of MDPC-23 cells. The population of S phase cells in *Nfic* small interfering RNA-inactivated MDPC-23 cells was increased by 13.41% compared with control cells, whereas the populations in the G_1 and G_2/M phases decreased, indicating S phase arrest (Fig. 5*B*).

p21-induced Cell Growth Arrest in Nfic-deficient Primary Pulp Cells—Cell cycle-related proteins and cyclin-dependent kinase inhibitors are known to regulate cell proliferation (35). To investigate whether any of these proteins are involved in the cell growth arrest caused by the loss of *Nfic*, the expression of p21, p16, cyclin D1, and cyclin B1 were examined in *Nfic*-deficient primary pulp cells by Western blot analysis. *Nfic*-deficient primary pulp cells exhibited an increase in p21 as well as p16 expression and a decrease in cyclin D1 as well as cyclin B1 expression compared with wild type cells (Fig. 5, *C* and *D*).

Apoptosis of Pulp Cells in Nfic-deficient Mice—To examine whether short root formation in *Nfic*-deficient mice is due to an
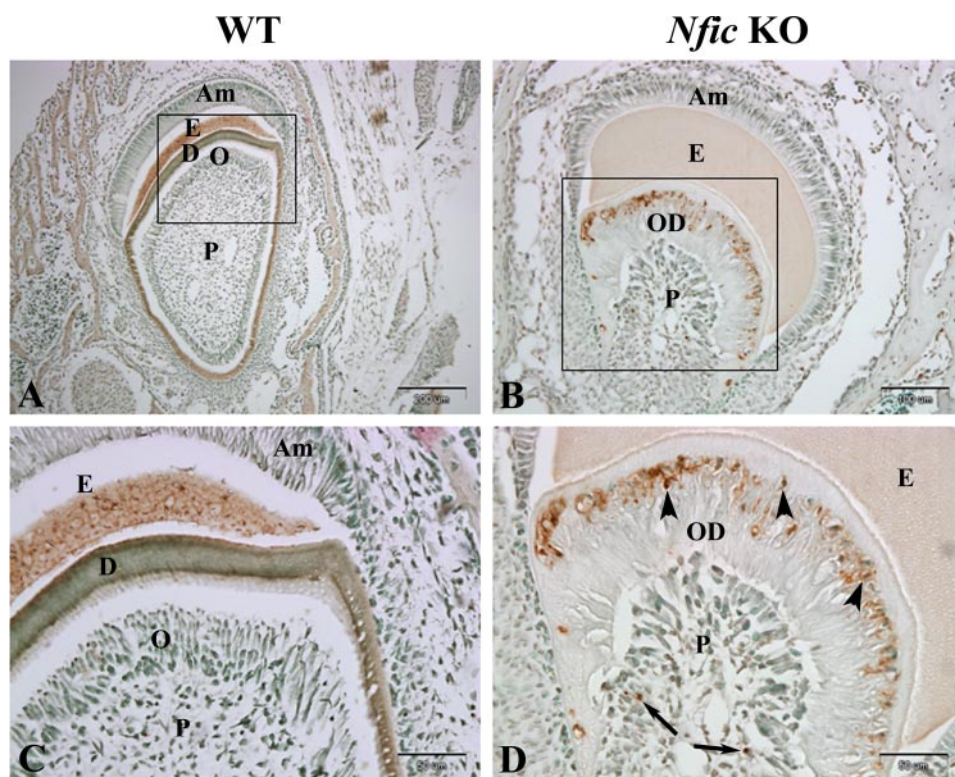
WT   *Nfic* KO

FIGURE 6. **Loss of the *Nfic* increased apoptotic activity in primary pulp cells.** TUNEL POD staining of P17 incisors from the wild type (*WT*, *A* and *C*) and *Nfic*-deficient mice (*B* and *D*). More TUNEL-positive cells were detected in the aberrant odontoblasts of *Nfic*-deficient mice compared with wild type mice. Apoptotic cells were detected in subodontoblastic cells (*arrows*) and were more numerous in the aberrant odontoblasts (*arrowheads*) trapped in abnormal dentin of *Nfic*-deficient mice. *C* and *D* show higher magnifications of *boxed A* and *B*, respectively. A cross-section is shown. *Am*, ameloblasts; *E*, enamel; *D*, dentin; *O*, odontoblasts; *OD*, osteodentin-like mineralized tissue; *P*, pulp. *Scale bars*, 100 μm; *B*, 50 μm; *C* and *D*, 20 μm.

increase in apoptosis of pulp cells and odontoblasts during root development, TUNEL POD staining in incisor histological sections from P17 wild type and *Nfic*-deficient mice was performed. Compared with wild type mice (Fig. 6, *A* and *C*), *Nfic*-deficient mice demonstrated an increase in apoptotic pulp cells, preodontoblastic cells in the subodontoblastic layer, and aberrant odontoblasts trapped in abnormal dentin (Figs. 6, *B* and *D*).

Apoptosis was Induced by Caspase Activation in Primary Pulp Cells of Nfic-deficient Mice—The expression of caspase-8 and -3, the central players of apoptosis, in *Nfic*-deficient primary pulp cells was examined by Western blot analysis. Both the expression and level of cleavage of caspase-8, known as the general initiator caspase, were higher in *Nfic*-deficient primary pulp cells compared with that of wild type cells (Fig. 7, *A* and *B*). Active caspase-8 can cleave and activate procaspase-3, which leads to apoptosis. The level of caspase-3 expression was also higher in *Nfic*-deficient primary pulp cells, and cleaved caspase-3 was detected in *Nfic*-deficient primary pulp cells (Fig. 7, *C* and *D*).

We next examined the expression of Bid, a mitochondria-related apoptosis effector that is cleaved by caspase-8 (36). The level of Bid expression was equivalent between wild type and *Nfic*-deficient primary pulp cells, and no Bid cleavage was detected (Fig. 7, *E* and *F*). The anti-apoptotic Bcl-2 family, including Bcl-2 and Bcl-X$_L$, was also examined by RT-PCR and Western blot analysis. The level of *Bcl-X*$_L$ remained unchanged, but the level of *Bcl-2* was higher in *Nfic*-deficient primary pulp

cells than wild type primary pulp cells (data not shown). xIAP and cIAP1/2 are direct caspase inhibitors and are known to bind to and inhibit activated caspase-3 and -7 and procaspase-9 (36). Western blot analysis showed that the expression level of cIAP1/2 was lower in *Nfic*-deficient primary pulp cells than controls (Fig. 7, *E* and *F*).

DISCUSSION

We previously reported that *Nfic*-deficient mice develop short roots with aberrant odontoblasts that exhibit unique morphological features (29). Unlike wild type odontoblasts, they display a rounded shape and lack the cellular polarization and organization normally seen in the odontoblast layer. Further, aberrant odontoblasts become dissociated and trapped in an osteodentin-like mineralized tissue. Interestingly, TGF-β1-overexpressing transgenic mice develop distinct dentin defects similar to those seen in *Nfic*-deficient mice (20). These transgenic animal studies strongly suggest a functional relationship between *Nfic* and *Smads* in odontoblast development. In the present study, *Nfic*-deficient mice demonstrated a higher expression level of TGFβ-RI and p-Smad2/3 than wild type mice. Furthermore, *Nfic*-deficient mice showed a decrease in DSP expression but an increase in BSP expression. This increase in BSP expression could indicate an altered differentiation state of the odontoblasts, where they have begun to take on some attributes of osteoblasts including BSP expression. Small interfering RNA inactivation of *Nfic* also increased BSP promoter activity. In addition, overexpression of Smad2 led to an up-regulation of BSP, whereas overexpression of Smad3 led to the down-regulation of BSP in MDPC-23 cells. It has previously been reported that Smad2 and Smad3 may play distinct roles in mediating TGF-β signaling in MDPC-23 cells (23). This led us to speculate that the increased TGF-β signaling observed in *Nfic*-deficient mice may be a direct result of the inactivation of the *Nfic* and is responsible for the aberrant odontoblasts and short root formation in *Nfic*-deficient mice. This hypothesis is supported by a recent study that compared the DNA-binding domains of *Smads* and NFI transcriptional factors (37). According to a sensitive PSI-Blast data base search, these transcriptional factors share significant similarities in their DNA-binding domains and may belong to a new superfamily of genes (38). The possible functional relationship between these two transcriptional factors in odontoblasts differentiation and functions during root formation is currently under investigation.

In the apical region of developing roots, both cervical loop and EM cells actively proliferate, and thus their well coordi-
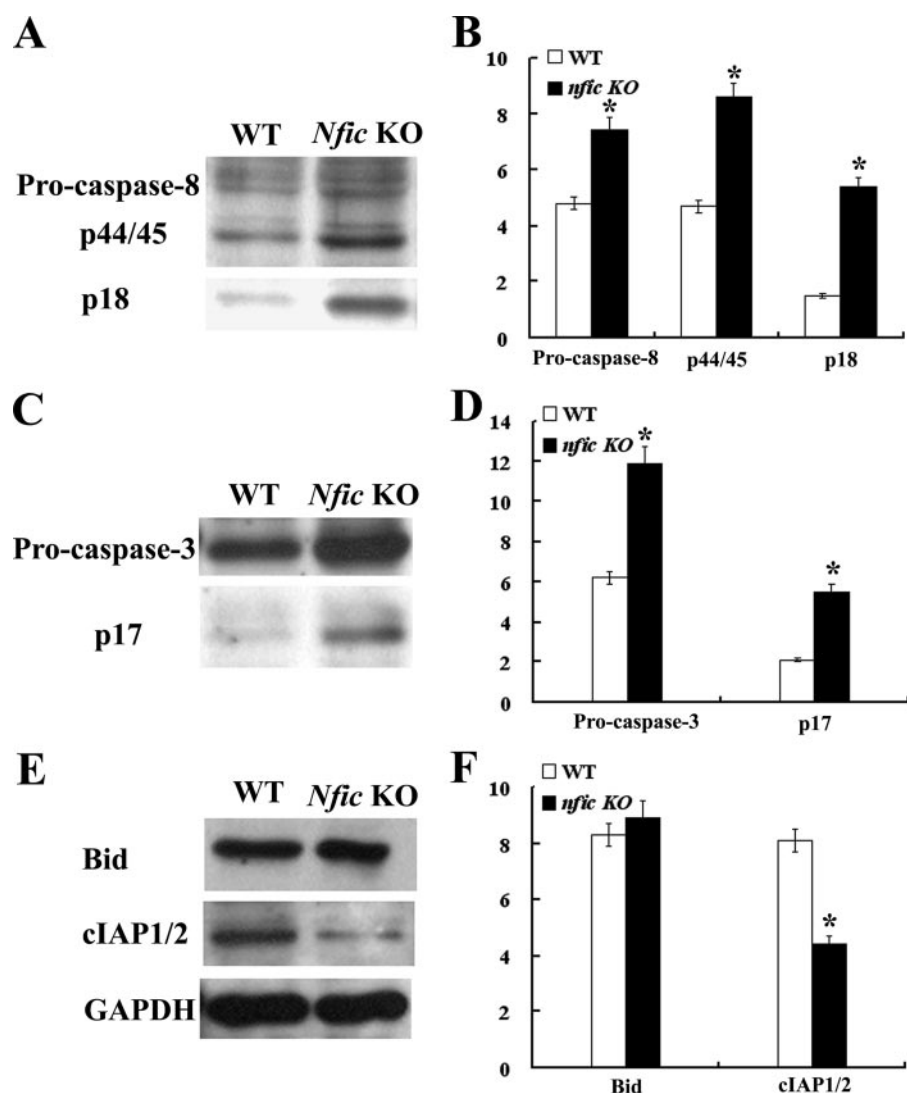
FIGURE 7. **Loss of *Nfic* induced apoptosis through the activation of caspases in primary pulp cells.** Evaluation of caspase-8 (*A* and *B*) and caspase-3 proteins (*C* and *D*) is shown. Evaluation of Bid and cIAP1/2 proteins (*E* and *F*) is shown. Whole cell lysates were obtained from primary pulp cells and separated by SDS-PAGE. Western blot analysis was carried out using anti-caspase-8, anti-caspase-3, anti-Bid, and anti-cIAP1/2 antibodies. The bands were measured by densitometric analysis of autoradiograph films (*B*, *D*, and *F*) (*, $p < 0.05$).

p21 has been shown to plays a key role in cell growth arrest at the G_1/S checkpoint by inhibiting the activity of cyclin E/Cdk2, cyclin D1/Cdk4/6, cyclin A/Cdk2, and, to a lesser extent, cyclin B/Cdc2 (35). Furthermore, p16 inhibits cyclin D/Cdk4/6 thereby preventing the inactivation of pRB (42). Interestingly, *Nfic* gene inactivation led to an increase in the expression of cell cycle inhibitors such as p21 and p16, which is in agreement with a recent finding that NFI is a key repressor of *p21* transcription (43). Further, TGF-β has been shown to inhibit cell cycle progression partially through the up-regulation of expression of p21, p15, and p27 cell cycle inhibitors (44). *Smads* also play an important role in the regulation of *p21* in HaCaT cells (45). These findings suggest that the loss of the *Nfic* gene may decrease the proliferation of cervical loop and EM cells through an increase in p21 expression and decrease in FGF10 expression in EM cells and may contribute in part to short root formation.

Apoptosis is an essential physiological process that plays a critical role in development and tissue homeostasis (46). During tooth development, apoptosis occurs at all stages: early tooth morphogenesis (47), amelogenesis (48), dentinogenesis (49), and tooth eruption (50). The specific temporospatial appearance of apoptotic cells during tooth development suggests its important role in odontogenesis

nated cell proliferation plays a crucial role in normal root formation (4). In particular, the EM cells adjacent to the cervical loop differentiate into odontoblasts that are responsible for root dentin formation. We found that *Nfic*-deficient mice had less BrdUrd-positive cervical loop and EM cells in the apical end of mandibular incisors than wild type mice. Previous studies showed that FGF10 plays a key role in the developing tooth by stimulating proliferation and differentiation of cervical loop stem cells (34, 39). It was reported that mouse incisors EM cells express FGF10, whereas its receptor, FGFR2b, is expressed throughout the cervical loop epithelium (34). In addition, the cervical loop of *Fgf*-deficient mice showed a decreased in cell proliferation. In the present study, *Nfic*-deficient primary pulp cells were shown to express a decreased level of *Fgf10* compared with wild type cells. Recently, it has been reported that TGF-β1 down-regulates *Fgf10* in the lung (40) and the prostate (41). Likewise, *Nfic*-deficient primary pulp cells showed a decrease in proliferation activity *in vitro* when compared with control cells.

(51). In the present study, the appearance of apoptotic cells was evident in the subodontoblastic region of developing roots from *Nfic*-deficient mice and more prominent in the area where aberrant odontoblasts trapped in abnormal dentin are located. However, little is known about the causes and signaling pathways responsible for odontoblast apoptosis. Previous studies showed that TGF-β1 induces apoptosis in MDPC-23 cells via a Smad-dependent pathway (23). Our findings suggest that inactivation of the *Nfic* leads to the up-regulation of TGF-β1 expression, which thereby induces the expression of Smad 2/3 in odontogenic cells. We therefore speculate that odontogenic cells in *Nfic*-deficient mice may undergo apoptosis via Smad-dependent pathways, resulting in short root formation.

Inhibitors of apoptosis (IAPs; cIAP1/2 and xIAP) are direct caspase inhibitors that bind to and inhibit active caspase-3 and -7, the key effectors of apoptosis (36). Recently, activated caspase-3 was detected in the primary enamel knot of the field vole (52), but little is known about the activation of other

caspases such as caspase-8 and -9. In the present study, the expression of caspase-8 and -3 was found to be increased, whereas c-IAP1/2 was decreased in *Nfic*-deficient primary pulp cells. It is known that the mitochondrial apoptotic pathway is initiated through caspase-8-mediated Bid cleavage (53), but we could not detect any cleaved form of Bid. However, even though the expression of *Bcl-X$_L$*, an anti-apoptotic member of the Bcl-2 family, remained unchanged, the expression of Bcl-2 was increased in *Nfic*-deficient primary pulp cells (data not shown). These findings suggest that procaspase-3, which is cleaved directly by activated caspase-8, but not by the mitochondrial apoptotic pathway, may also be involved in apoptosis of *Nfic*-deficient primary pulp cells.

In the present study, wild type mice exhibited normal circular dentin, but *Nfic*-deficient mice contained abnormal dentin, osteodentin. In *Nfic*-deficient mice, the labial side of an incisor exhibited osteodentin, whereas the lingual side showed an open area of the dentin because of the lack of dentin formation. Dentin is covered by enamel and ameloblast in the labial side of an incisor, whereas it is not covered in the lingual side. Interestingly, ameloblast-lineage cell-conditioned media facilitated the differentiation and mineralization of MDPC-23 cells compared with their control counterparts (data not shown). Ameloblast-lineage cell-conditioned media also affected the expression of NFI-C during odontoblast differentiation (data not shown). Therefore, these results suggest a link between ameloblasts and odontoblasts during tooth development, through NFI-C. This speculation requires further investigation. In conclusion, NFI-C appears to play an important role in the proliferation of odontogenic cells, their differentiation into odontoblasts, and odontoblasts survival during root formation. Therefore, inactivation of the *Nfic* gene may result in short root formation.

REFERENCES

1. Smith, A. J., and Lesot, H. (2001) *Crit. Rev. Oral Biol. Med.* **12,** 425–437
2. Sharpe, P. T. (2001) *Adv. Dent. Res.* **15,** 4–7
3. Zeichner-David, M., Oishi, K., Su, Z., Zakartchenko, V., Chen, L. S., Arzate, H., and Bringas, P., Jr. (2003) *Dev. Dyn.* **228,** 651–663
4. Kaneko, H., Hashimoto, S., Enokiya, Y., Ogiuchi, H., and Shimono, M. (1999) *Cell Tissue Res.* **298,** 95–103
5. Luan, X., Ito, Y., and Diekwisch, T. G. (2006) *Dev. Dyn.* **235,** 1167–1180
6. Nagata, K., Guggenheimer, R. A., Enomoto, T., Lichy, J. H., and Hurwitz, J. (1982) *Proc. Natl. Acad. Sci. U. S. A.* **79,** 6438–6442
7. Gronostajski, R. M. (2000) *Gene* **249,** 31–45
8. Chaudhry, A. Z., Lyons, G. E., and Gronostajski, R. M. (1997) *Dev. Dyn.* **208,** 313–325
9. Shu, T., Butz, K. G., Plachez, C., Gronostajski, R. M., and Richards, L. J. (2003) *J. Neurosci.* **23,** 203–212
10. Steele-Perkins, G., Plachez, C., Butz, K. G., Yang, G., Bachurski, C. J., Kinsman, S. L., Litwack, E. D., Richards, L. J., and Gronostajski, R. M. (2005) *Mol. Cell. Biol.* **25,** 685–698
11. Gründer, A., Ebel, T. T., Mallo, M., Schwarzkopf, G., Shimizu, T., Sippel, A. E., and Schrewe, H. (2002) *Mech. Dev.* **112,** 69–77
12. Driller, K., Pagenstecher, A., Uhl, M., Omran, H., Berlis, A., Gründer, A., and Sippel, A. E. (2007) *Mol. Cell. Biol.* **27,** 3855–3867
13. Steele-Perkins, G., Butz, K. G., Lyons, G. E., Zeichner-David, M., Kim, H. J., Cho, M. I., and Gronostajski, R. M. (2003) *Mol. Cell. Biol.* **23,** 1075–1084
14. Lee, K. Y., and Bae, S. C. (2002) *J. Biochem. Mol. Biol.* **35,** 47–53
15. Siegel, P. M., and Massagué, J. (2003) *Nat. Rev. Cancer* **3,** 807–821
16. Sánchez-Capelo, A. (2005) *Cytokine Growth Factor Rev.* **16,** 15–34
17. Schuster, N., and Krieglstein, K. (2002) *Cell Tissue Res.* **307,** 1–14
18. Miyazono, K., Kusanagi, K., and Inoue, H. (2001) *J. Cell. Physiol.* **187,** 265–276
19. Smith, A. J., Matthews, J. B., and Hall, R. C. (1998) *Eur. J. Oral Sci.* **106,** (Suppl. 1) 179–184
20. Thyagarajan, T., Sreenath, T., Cho, A., Wright, J. T., and Kulkarni, A. B. (2001) *J. Biol. Chem.* **276,** 11016–11020
21. Hanks, C. T., Sun, Z. L., Fang, D. N., Edwards, C. A., Wataha, J. C., Ritchie, H. H., and Butler, W. T. (1998) *Connect. Tissue Res.* **37,** 233–249
22. Sun, Z. L., Fang, D. N., Wu, X. Y., Ritchie, H. H., Bègue-Kirn, C., Wataha, J. C., Hanks, C. T., and Butler, W. T. (1998) *Connect. Tissue Res.* **37,** 251–261
23. He, W. X., Niu, Z. Y., Zhao, S. L., and Smith, A. J. (2005) *Arch. Oral Biol.* **50,** 929–936
24. Hwang, Y. C., Hwang, I. N., Oh, W. M., Park, J. C., Lee, D. S., and Son, H. H. (2008) *J. Mol. Histol.* **39,** 153–160
25. Park, J. C., Herr, Y., Kim, H. J., Gronostajski, R. M., and Cho, M. I. (2007) *J. Periodontol.* **78,** 1795–1802
26. Couble, M. L., Farges, J. C., Bleicher, F., Perrat-Mabillon, B., Boudeulle, M., and Magloire, H. (2000) *Calcif. Tissue Int.* **66,** 129–138
27. Smith, A. J., Tobias, R. S., Plant, C. G., Browne, R. M., Lesot, H., and Ruch, J. V. (1990) *J. Biol. Buccale* **18,** 123–129
28. Butler, W. T. (1998) *Eur. J. Oral Sci.* **106,** (Suppl. l) 204–210
29. zur Nieden, N. I., Kempka, G., and Ahr, H. J. (2003) *Differentiation* **71,** 18–27
30. Unterbrink, A., O'Sullivan, M., Chen, S., and MacDougall, M. (2002) *Connect. Tissue Res.* **43,** 354–358
31. Miyazaki, T., Kanatani, N., Rokutanda, S., Yoshida, C., Toyosawa, S., Nakamura, R., Takada, S., and Komori, T. (2008) *Arch. Histol. Cytol.* **71,** 131–146
32. He, W. X., Niu, Z. Y., Zhao, S. L., Jin, W. L., Gao, J., and Smith, A. J. (2004) *Arch. Oral Biol.* **49,** 911–918
33. Ogata, Y., Niisato, N., Furuyama, S., Cheifetz, S., Kim, R. H., Sugiya, H., and Sodek, J. (1997) *J. Cell. Biochem.* **65,** 501–512
34. Harada, H., Toyono, T., Toyoshima, K., Yamasaki, M., Itoh, N., Kato, S., Sekine, K., and Ohuchi, H. (2002) *Development* **129,** 1533–1541
35. Shackelford, R. E., Kaufmann, W. K., and Paules, R. S. (2000) *Free Radic. Biol. Med.* **28,** 1387–1404
36. Philchenkov, A. A. (2003) *Biochemistry* **68,** 365–376
37. Stefancsik, R., and Sarkar, S. (2003) *DNA Sequence* **14,** 233–239
38. Iozzo, R. V., Pillarisetti, J., Sharma, B., Murdoch, A. D., Danielson, K. G., Uitto, J., and Mauviel, A. (1997) *J. Biol. Chem.* **272,** 5219–5228
39. Yokohama-Tamaki, T., Ohshima, H., Fujiwara, N., Takada, Y., Ichimori, Y., Wakisaka, S., Ohuchi, H., and Harada, H. (2006) *Development* **133,** 1359–1366
40. Chen, F., Desai, T. J., Qian, J., Niederreither, K., Lü, J., and Cardoso, W. V. (2007) *Development* **134,** 2969–2979
41. Tomlinson, D. C., Grindley, J. C., and Thomson, A. A. (2004) *Endocrinology* **145,** 1988–1995
42. Cox, L. S. (1997) *J. Pathol.* **183,** 134–140
43. Ouellet, S., Vigneault, F., Lessard, M., Leclerc, S., Drouin, R., and Guérin, S. L. (2006) *Nucleic Acids Res.* **34,** 6472–6487
44. Gong, J., Ammanamanchi, S., Ko, T. C., and Brattain, M. G. (2003) *Cancer Res.* **63,** 3340–3346
45. Pardali, K., Kurisaki, A., Morén, A., ten Dijke, P., Kardassis, D., and Moustakas, A. (2000) *J. Biol. Chem.* **275,** 29244–29256
46. Schultz, D. R., and Harrington, W. J., Jr. (2003) *Semin. Arthritis Rheum.* **32,** 345–369
47. Shigemura, N., Kiyoshima, T., Kobayashi, I., Matsuo, K., Yamaza, H., Akamine, A., and Sakai, H. (1999) *Histochem. J.* **31,** 367–377
48. Bronckers, A. L., Goei, S. W., Dumont, E., Lyaruu, D. M., Wöltgens, J. H., van Heerde, W. L., Reutelingsperger, C. P., and van den Eijnde, S. M. (2000) *Histochem. Cell Biol.* **113,** 293–301
49. Vermelin, L., Lécolle, S., Septier, D., Lasfargues, J. J., and Goldberg, M. (1996) *Eur. J. Oral Sci.* **104,** 547–553
50. Ten Cate, A. R., and Anderson, R. D. (1986) *J. Dent. Res.* **65,** 1087–1093
51. Matalova, E., Tucker, A. S., and Sharpe, P. T. (2004) *J. Dent. Res.* **83,** 11–16
52. Shigemura, N., Kiyoshima, T., Sakai, T., Matsuo, K., Momoi, T., Yamaza, H., Kobayashi, I., Wada, H., Akamine, A., and Sakai, H. (2001) *Histochem. J.* **33,** 253–258
53. Zimmermann, K. C., Bonzon, C., and Green, D. R. (2001) *Pharmacol. Ther.* **92,** 57–70